

## Processes driving thunderstorms over the Agulhas Current

Agatha M. de Boer,<sup>1,2</sup> Andrew B. Collier,<sup>3,4</sup> and Rodrigo Caballero<sup>5,2</sup>

Received 26 July 2012; revised 28 January 2013; accepted 30 January 2013.

[1] Lightning occurs predominantly over land and is not common over the open ocean. We study here one oceanic region in which thunderstorms are frequently found, namely the warm Agulhas Current off the southeast coast of South Africa. The seasonal and interannual lightning variability is derived from satellite and terrestrial data sets. Favorable climatic conditions for lightning are investigated using both ERA-Interim and NCEP/NCAR reanalysis data. We find peak lightning in austral autumn over the Agulhas Current but with low seasonality (i.e., there is considerable lightning throughout the year). While the climatological wind direction varies strongly with latitude and season, the wind direction is predominantly northerly throughout the region during thunderstorms. A composite of sea level pressure during thunderstorm days indicates that thunderstorms are related to eastward-propagating synoptic-scale wave trains passing through the Agulhas Current region. The strong convective activity during thunderstorms occur in the warm sector of a cyclone and is associated with horizontal convergence and lifting of warm, moist surface air originating over the warm Agulhas Current.

**Citation:** de Boer, A. M., A. B. Collier, and R. Caballero (2013), Processes driving thunderstorms over the Agulhas Current, *J. Geophys. Res. Atmos.*, 118, doi:10.1002/jgrd.50238.

### 1. Introduction

[2] Lightning over the ocean occurs much less frequently than over land [Cecil *et al.*, 2005; Christian *et al.*, 2003; Mackerras *et al.*, 1998; Williams and Stanfill, 2002]. One of the few regions of intense oceanic lightning is over the Agulhas Current off the east coast of South Africa and its retroflexion toward the Indian Ocean (Figure 1). The Agulhas Current is a warm western boundary current and supports some of the highest air sea fluxes in the world [Beal *et al.*, 2011; Jury and Walker, 1988; Rouault *et al.*, 2000; Rouault *et al.*, 1995]. The intense moist convection that generates lightning may have important effects on the large-scale environment, so that understanding the processes that drive it can contribute to an understanding of the atmospheric general circulation. Lightning over this region is also of interest to space physicists. The lightning strokes produce whistlers that are detected in Tihany, Hungary (the Northern Hemisphere conjugate point for the Agulhas Current region) and the detected signal gives information about the magnetosphere [Collier *et al.*, 2006]. It appears that whistlers are

more often produced by oceanic lightning than adjacent continental lightning. Understanding the differences between the formation of the lightning over the Agulhas Current and the adjacent land will aid in interpreting the whistler frequencies.

[3] Midlatitude lightning over the ocean has been associated with deep convective clouds that develop around cyclones and their attendant fronts [Dirks *et al.*, 1988; Kodama *et al.*, 2007]. The Agulhas Current region lies on the northern boundary of the Southern Hemisphere storm track [Hoskins and Hodges, 2005; Inatsu and Hoskins, 2004]. Deep cyclones in the storm track, particularly cut-off lows, can cause heavy rainfall over the region [Singleton and Reason, 2007]. Another typical feature of the region is coastal lows, small-scale low-pressure systems that develop off the South African coast due to interaction between the large-scale airflow and the topography of the South African plateau. These coastal lows then propagate eastward [Reason and Jury, 1990]. The warm sea surface temperature of the Agulhas Current region has a strong influence on the asymmetry of the Southern Hemisphere storm track and increases the local cyclonic activity [Inatsu and Hoskins, 2004; Reason, 2001]. Czaja and Bhunt [2011] found that western boundary currents—including the Agulhas—and their extensions into the open ocean are favored sites for the development of deep convection. They argue that this is because of the poleward advection of warm water in the western boundary currents that generates regions of strong atmosphere-ocean disequilibrium, favoring heating and moistening at the base of the air column and leading to convective instability.

[4] Here the focus is specifically on the cause of the high lightning occurrence over the Agulhas Current region. Until recently there have been only sparse observations of

<sup>1</sup>Department of Geological Science, Stockholm University, 106 91, Stockholm, Sweden.

<sup>2</sup>Bert Bolin Centre for Climate Research, Stockholm University, Stockholm, Sweden.

<sup>3</sup>SANSA Space Science, Hermanus, 7200, South Africa.

<sup>4</sup>School of Chemistry and Physics, University of KwaZulu-Natal, Durban, 4000, South Africa.

<sup>5</sup>Department of Meteorology, Stockholm University, 106 91, Stockholm, Sweden.

Corresponding author: A. M. de Boer, Department of Geological Science, Stockholm University, 106 91 Stockholm, Sweden. (agatha.deboer@geo.su.se)

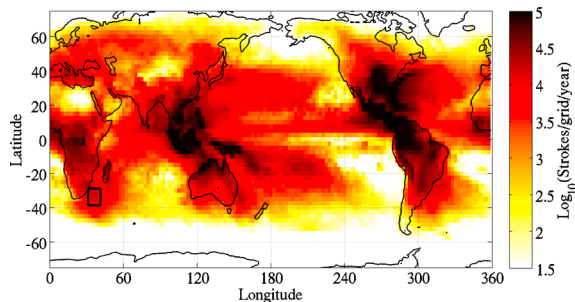


**Figure 1.** Global distribution of lightning density as detected by the World Wide Lightning Location Network (WWLLN). The density is the mean number of lightning strokes in each  $2.5^\circ \times 2.5^\circ$  grid box per year for the analysis period 2005 to 2011. The small black box off the east coast of southern Africa indicates the Agulhas Current region for which the lightning occurrence is analyzed in this study.

lightning in coastal areas and almost no observations over the open ocean. Two advances in lightning detection have changed this: satellite detection and global terrestrial networks like the World Wide Lightning Location Network (WWLLN) [Dowden *et al.*, 2008; Virts *et al.*, 2013]. In the past, lightning observations relied on land-based detectors, which measured high-frequency radio pulses from lightning that do not travel very far. The instruments were more common in developed areas with high population density. Lightning is now routinely measured by satellites, which do not discriminate in detection efficiency between land and ocean. The VLF radio signals emitted by lightning are utilized by WWLLN to pinpoint lightning position by triangulation. In this study we make use of both these relatively new lightning data sources in conjunction with climate variables from atmospheric reanalysis data sets to understand the characteristics of and mechanisms that drive lightning over the Agulhas Current.

[5] The data sources and methods are described in section 2. In section 3 we describe first the temporal distribution of lightning and then relate lightning frequency to the wind strength and direction, the sea level pressure, and surface air temperature. The analysis of average conditions for lightning is followed by two case studies of strong thunderstorms in section 4. Finally, we discuss our results and draw conclusions in section 5.

## 2. Data and Methodology

[6] Two distinct yet complementary lightning observation methods are used in this analysis. The first type, for which data from 1996–2007 are used, is lightning detected by the Lightning Imaging Sensor (LIS) and the Optical Transient Detector (OTD) satellite instruments. OTD was operational from May 1995 until March 2000, while LIS has been active from November 1997 until the present. The two satellite data sets have a very high efficiency: essentially all lightning strokes are detected, but only within the satellite’s field of view. The satellites typically observe a given location at the same local time once every 20 to 40 days, depending on latitude. Due to the nature of satellite observations, a given location is only covered intermittently, if at all. The

spatial resolution of OTD and LIS are about 8 and 4 km, respectively [Boccippio *et al.*, 2000; Christian *et al.*, 2000].

[7] The second type of lightning data is derived from a global network of WWLLN VLF receivers. The data span the period 2005–2011 and provide continuous coverage of the entire globe. Between 2005 and 2011 the number of WWLLN receivers has more than doubled and the algorithm used to assimilate the data from the various stations in the network has been refined and improved. As a result the efficiency of the network increased from 2.8% to 11.1% [Rodger *et al.*, 2009]. The location of a stroke is accurately measured to within about 10 km. The WWLLN data set is therefore well suited to indicating whether or not there is lightning activity in a given region, but does not capture every discharge and is not suitable for interannual comparisons. By contrast, LIS and OTD detect the majority of lightning discharges but only within their respective fields of view. The LIS/OTD data are used here to study the seasonal and interannual variability of the lightning using principal component analysis (PCA) while the WWLLN data are used to determine the spatial and temporal distribution of the lightning and for a comparison with climate variables such as wind and sea level pressure.

[8] The WWLLN and the LIS/OTD data were binned daily and projected onto a  $2.5^\circ$  latitude  $\times$   $2.5^\circ$  longitude grid to correspond with that of the National Centers for Environmental Prediction (NCEP) and the National Centre for Atmospheric Research (NCAR) reanalysis data (see below). The Agulhas Current region defined for the present analysis extends from  $31.25^\circ\text{E}$  to  $41.25^\circ\text{E}$  and  $28.75^\circ\text{S}$  to  $38.75^\circ\text{S}$  and covers 16 grid boxes (black box in Figure 1). The environmental data used in the climatological analysis of section 3 are from the NCEP/NCAR reanalysis 1 [Kalnay *et al.*, 1996]. The variables used are the zonal and meridional winds, air temperature at the sigma 0.995 level ( $\sim 40$  m above sea level), and sea level pressure. In addition, in section 4 we study the evolution of environmental conditions during two selected high-lightning events using the ERA-Interim reanalysis data set [Dee *et al.*, 2011] which with its finer  $0.75^\circ$  horizontal resolution is better suited to this type of analysis.

## 3. Results

### 3.1. Temporal Distribution of Lightning

[9] The LIS/OTD data cover a longer period than the WWLLN data and were therefore chosen as the optimum data set to use for a PCA [Green and Carroll, 1978; Mardia *et al.*, 1979] of the regional lightning around the Agulhas Current. PCA is used to determine the dominant modes of temporal variability and the spatial regions in which these apply. The analysis was performed on monthly average lightning flash rate densities for each cell. When applied to the lightning data, the first three principal components (PCs) accounted for 62.0%, 14.2% and 8.2% of the variance respectively, yielding a total of 84.4%, which is an appreciable fraction of the total variance in the data. It is thus reasonable to assume that the dominant variations are captured by the leading three PCs. The first three PC signals and their corresponding loadings are displayed in Figure 2. The variability associated with each mode is the product of the PC signal and the spatial loading pattern. The ranges of the PCs in Figure 2 appear to be rather large, however, these

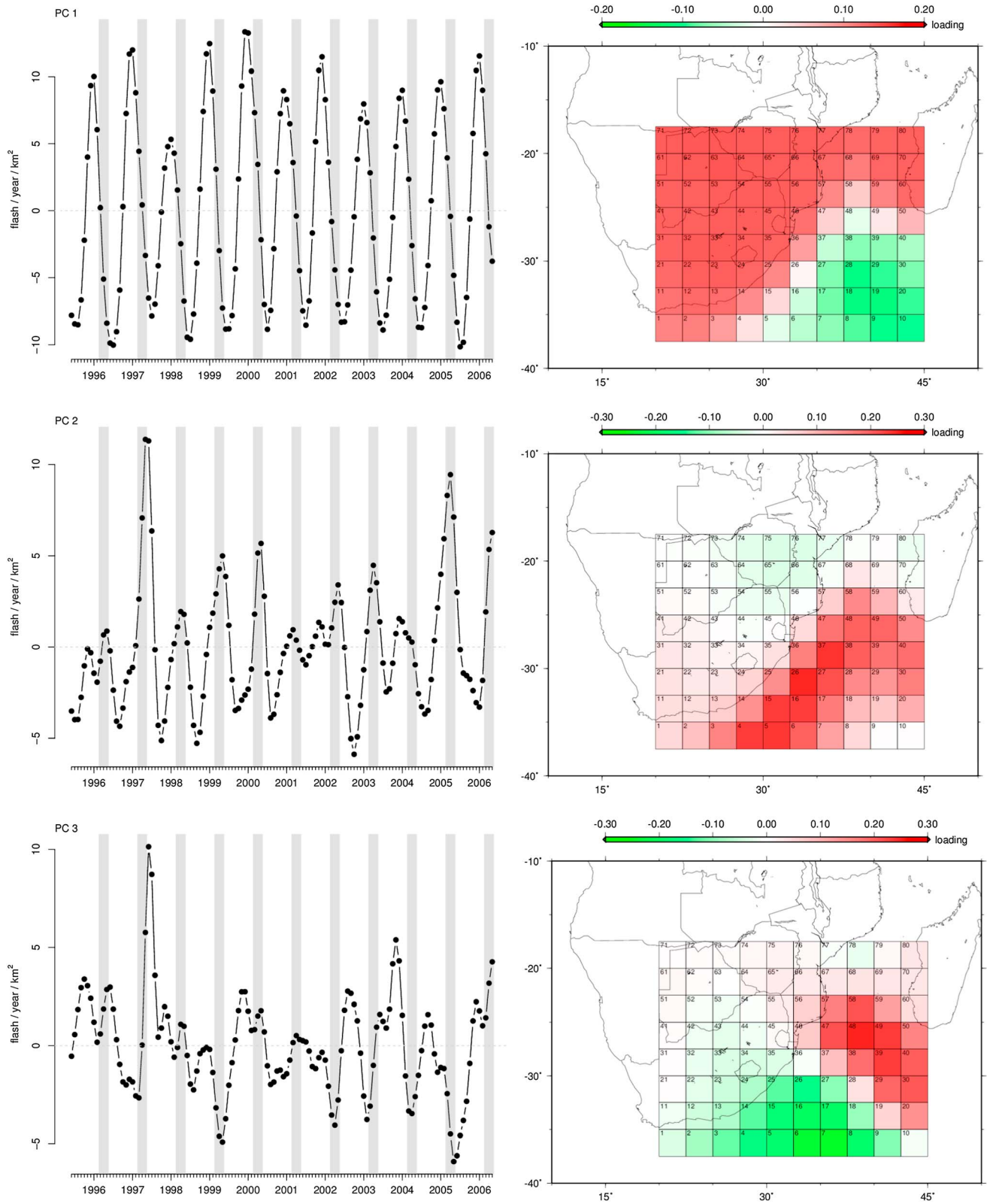


**Figure 2.** The first three principal component time series (left) and the corresponding weighting patterns (right) for lightning in the Agulhas Current region and adjacent land area. The lightning data are from the LIS/ODT satellites for the period 1996 to 2007. These first three principal components account for 62.0%, 14.2%, and 8.2% of the variance respectively. The vertical grey bands in the time series indicate the months of autumn.

must be considered in conjunction with the loadings, which are relatively small. The first component, PC1, represents a signal with a regular annual variation and a well-defined peak which usually occurs during summer. The spatial loading pattern in Figure 2a indicates that cells over South Africa and Madagascar are positively correlated with PC1. This is consistent with the fact that peak lightning activity over land normally occurs during the summer months. The second component, PC2, also displays a clear annual variation which peaks during austral autumn. This variation is, however, quite irregular, exhibiting significant interannual variability. The loadings in Figure 2b show that this behavior is most prevalent over the ocean east of South Africa. Portions of Southern Africa and Madagascar are anticorrelated with PC2. Finally, although PC3 displays some evidence of annual and semi-annual variations, the temporal structure is appreciably less regular than the foregoing PCs. The spatial structure suggests a weak bipolar mode of variability in which the northeast and southwest oceanic regions are out of phase.

[10] A complementary method of assessing the seasonal variability of lightning is to determine the most likely period of the year for lightning at each spatial point. For that purpose the 7 years of WLLN data were binned into six bimonthly intervals, i.e., December–January, February–March, April–May, June–July, August–September, and October–November. These six periods were chosen as a compromise between the options of using only four seasonal bins, which results in loss of temporal resolution, and using 12 monthly bins, which is difficult to represent in only a few spatial plots. Over land the months of peak lightning are the warmest summer months of December–January (Figure 3a). Over most of the Agulhas Current region the peak lightning occurs in April–May (Figure 3a). At higher latitudes ( $\sim 37^\circ\text{S}$  to  $50^\circ\text{S}$ ) there is a tendency for lightning later in the year (June–July and August–September) although it should be noted that the absolute lightning density is lower at these latitudes (Figure 1).

[11] There is a clear evidence for peak summer lightning over the continent and autumn lightning over the Agulhas Current. To determine the strength of this seasonality we calculated the percentage of lightning in the peak two month period at each gridpoint (Figure 3b). A much higher percentage of lightning occurs in the peak two months over the continent than over the ocean, which indicates that lightning is a much more seasonal phenomenon over land. While the Agulhas Current region receives 31% of its lightning in the

peak period, but 8% in the weakest period, a similar size region over continental Southern Africa (between  $21.25^\circ\text{E}$  to  $31.25^\circ\text{E}$  and  $38.75^\circ\text{S}$  to  $28.75^\circ\text{S}$ ) receives 51% of its lightning in the peak period and no lightning in the weakest period. During the summer South Africa experiences a variety of thunderstorms from single cell to mesoscale convective complexes and occasional extratropical cyclones [Blamey and Reason, 2009; 2012; Reason and Keibel, 2004; Tyson and Preston-Whyte, 2000], but in winter there is no source of moisture to support the development of thunderstorms [Dyson, 2009; Taljaard, 1996]. The conditions for oceanic lightning, while certainly seasonal, are therefore not as strongly bound to a specific season as the continental lightning.

### 3.2. Climatological Conditions for Lightning

#### 3.2.1. Wind Direction

[12] The Agulhas Current region lies between the climatological midlatitude westerlies and the subtropical easterlies, so that the mean winds in the region depend strongly on latitude and season. To assess the difference between the climatological wind direction and the direction during thunderstorms, we split the Agulhas box indicated in Figure 1 into a northern and southern half (Figure 4). Seasons are represented in color on the wind rose. In the northern, lower-latitude Agulhas Current region ( $28.72^\circ\text{S}$ – $33.75^\circ\text{S}$ ) the climatological winds range from southerly to easterly to northerly while in the southern, higher-latitude Agulhas region ( $33.75^\circ\text{S}$ – $38.75^\circ\text{S}$ ) the winds are more omnidirectional but show a clear preference for westerly to northerly winds (Figures 4a and 4c). A semipermanent high pressure in the South Indian Ocean leads to the frequent northerly winds in the region. On days of thunderstorms (which we define as having at least 10 lightning strokes in the gridbox during the day) the winds show a strong northerly pattern which is shifted slightly to the east in the lower latitude half and shifted to the west in the higher latitude half. No lightning occurs at higher latitudes for southerly winds. The structure of the wind pattern is not very sensitive to the cut-off of 10 strokes per day but tends to exhibit a stronger northerly wind structure for a higher cut off (not shown). Although the prevailing winds are a little more westerly during austral winter than summer, there is no obvious difference in the wind direction associated with thunderstorms between the different seasons.

#### 3.2.2. Sea-Level Pressure, Wind, and Temperature

[13] The average sea level pressure (SLP) pattern during thunderstorms is determined through a composite of the

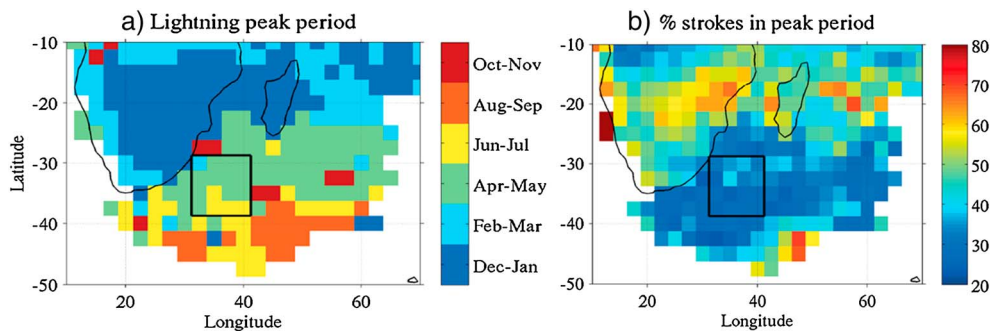


**Figure 3.** The bimonthly period in which the lightning peaks (a) and percentage of annual lightning that falls in that period (b). Areas which receive less than 1000 strokes per year per  $2.5^\circ \times 2.5^\circ$  box are masked out. The black rectangle is the Agulhas Current region evaluated in Figure 4.

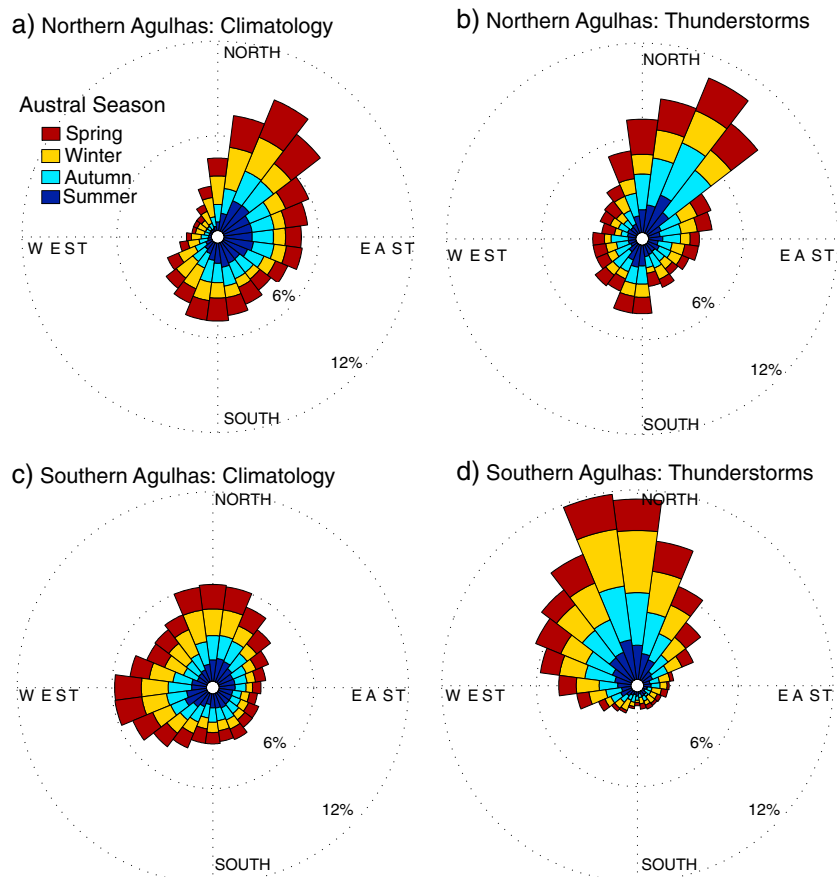


**Figure 4.** The distribution of wind direction in (a,b) the northern half and (c,d) southern half of the Agulhas Current region (indicated by the black box in Figures 1 and 3). To the left (Figures 4a and 4c) are the wind climatologies and to the right (Figures 4b and 4d) are the distributions for days in which there were more than 10 strokes in a given grid box (the conclusions are not sensitive to this cut-off value). The angle is the direction from which the wind blows so that the winds are directed toward the center of the diagrams. The color indicates the austral seasons, namely: summer (DJF), autumn (MAM), winter (JJA), spring (SON).

SLP anomaly (i.e., with the monthly mean subtracted) over the southern Indian Ocean during days when there are more than a total of 100 strokes in the whole Agulhas Current region (Figure 5b). The composite reveals a clear low-pressure center spanning the region that is part of a wave train with a dominant zonal wave number of 5 or 6 (around  $60\text{--}70^\circ$  wavelength). Lag composites 2 days before and after the selected day (Figures 5a and 5b) suggest that the wave train is moving eastward. These features are consistent with the well-known tendency for synoptic eddies to organize into zonally propagating wave packets in the southern hemisphere storm track [Lee and Held, 1993; Chang, 2000]. Note that high lightning activity occurs when the phase of the wave packet is such that a cyclone lies on or slightly west of the region while an anticyclone of similar intensity lies to the east. The results are insensitive to the 100 strokes per day cut-off: using a 1000 strokes cut-off but extending the colorbar limits to  $\pm 400$  Pa (instead of  $\pm 200$  Pa) yields maps that are almost indistinguishable (not shown).

[14] Figure 6 shows a composite of near-surface air temperature and wind anomalies during days of high lightning activity over the Agulhas Current region. The cyclone-anticyclone couplet noted in Figure 5b brings warm northerly

winds over the central and eastern parts of the Agulhas Current region; at the same time, southwesterly advection around the cyclone brings cold air over the continent and the western part of the Agulhas Current region. These two airstreams meet at a clearly-defined cold front stretching northwest-southeast over South Africa and into the Agulhas current region. These results are consistent with the classical picture of thunderstorms occurring in the rising “warm conveyor belt” (WCB) within the cyclone’s warm sector [Browning, 1986].

#### 4. Individual Case Studies

[15] The climatological analysis of the previous section generally indicates a central role for synoptic-scale cyclones and associated fronts in generating lightning activity over the Agulhas Current region. To gain further insight, we examine two specific cases in greater detail. The storms occurred on 14 May 2011 and 15 October 2011. These two days have among the highest incidences of lightning in the WLLN data set, with respectively 12,437 and 13,780 strokes occurring in the Agulhas Current region over the specified day. The analysis below was performed for a larger sample of high-lightning days; the two cases presented here

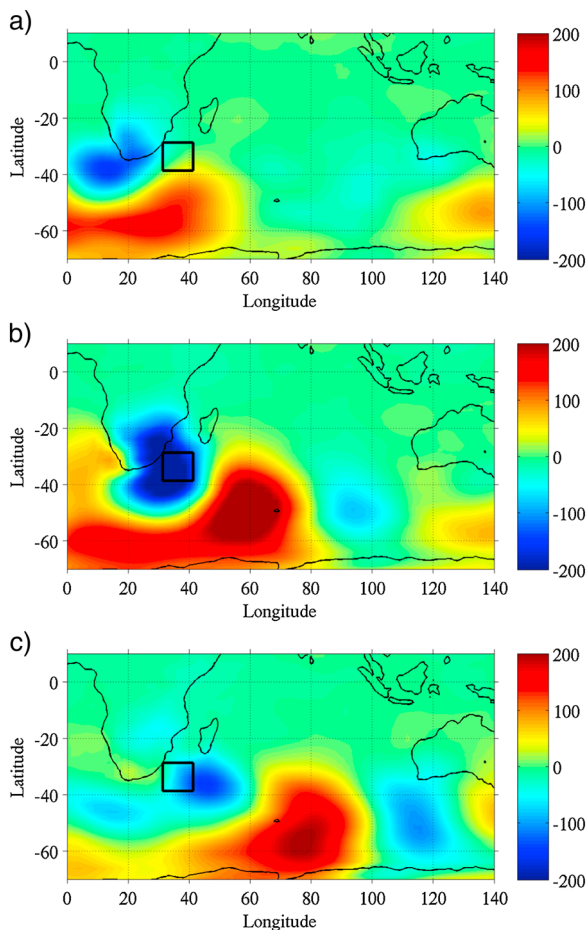


**Figure 5.** Composite of the sea level pressure anomaly (in units of Pa) (a) two days prior to a high lightning activity in the Agulhas Current region, (b) on the day of high lightning activity, and (c) two days after high lightning activity. A day with high lightning activity is defined as a day when more than 100 strokes occurred in the black rectangle box noted in the figure. The relevant monthly climatological sea level pressure field was subtracted from all the data points before the composites were taken.

were selected because they are representative of the different “flavors” of cyclone phenomenology associated with intense lightning.

#### 4.1. Cut-Off Low (15 October 2011)

[16] The first case (left column of Figure 7) is a classical cut-off low, often associated with severe weather in this region [Singleton and Reason, 2007]. To represent the upper-level flow, we use the potential temperature field on the 2 PVU (potential vorticity unit) surface,  $\theta_{PV2}$  ( $1 \text{ PVU} \equiv 10^6 \text{ m}^2 \text{ s}^{-1} \text{ K kg}^{-1}$ ), which is a good approximation to the tropopause elevation for air originating poleward of  $25^\circ$  latitude and compactly summarizes the important upper-level dynamical information. Low  $\theta_{PV2}$  implies a depressed tropopause and a positive (i.e., cyclonic) potential vorticity anomaly, and vice-versa for high  $\theta_{PV2}$ . Southwest of the Agulhas Current region in Figure 7a we see an extrusion of low- $\theta_{PV2}$  polar air whose tip has become detached, apparently through cyclonic Rossby wave breaking

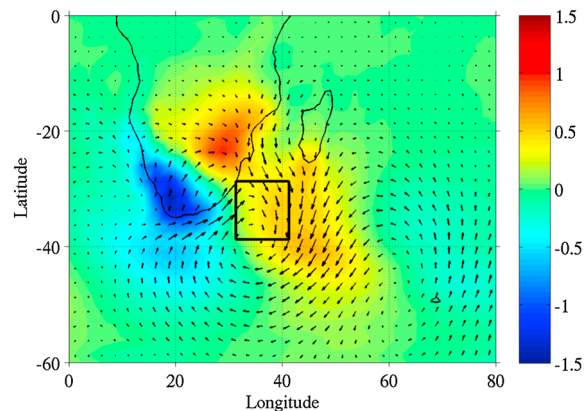


**Figure 6.** Composite of the NCEP/NCAR reanalysis surface air temperature anomalies (shading, units of K) and surface wind field (arrows) for days in which more than 100 strokes occurred in the Agulhas Current region box noted with the black rectangle. Monthly climatological temperature and wind fields were subtracted from all the data points before the composites were taken.

[Thorncroft *et al.*, 1993], leaving an isolated patch of cyclonic vorticity near the southwest corner of the Agulhas Current region. The 500 hPa height field (not shown) exhibits closed contours at this location, qualifying this system as a cut-off low. To the east of the region there is a strong and broad poleward incursion of subtropical, high- $\theta_{PV2}$  air and associated anticyclonic vorticity.

[17] These upper-level potential vorticity anomalies are matched at the surface (Figure 7b) by a deep low-pressure center south of the Agulhas Current region and a broad anticyclone to the east. The thermodynamic properties of the near-surface air are represented here by the equivalent potential temperature  $\theta_e$ , a quantity whose logarithm is proportional to the total entropy of the air including the latent heat contribution and which increases monotonically as a function of both temperature and humidity. As in the composite discussed in the previous section (Figure 5b), a well-developed cold front can be clearly identified in the  $\theta_e$  field, trailing northwestward out of the surface cyclone, across the target region and over South Africa. Northerly jet-like winds duct a narrow stream of high- $\theta_e$  air parallel to the cold front, a feature identifiable as the WCB associated with this cyclone. The region of intense lightning activity (grey shading in Figure 7b) is embedded within the WCB.

[18] A vertical section parallel to the WCB (Figure 7c) shows the northerly low-level winds advecting high- $\theta_e$  air southward and then rising sharply in the area coincident with the high lightning activity. Outgoing longwave radiation in the lightning region shows brightness temperatures of about 260 K, which given the local temperature profile indicates cloud-top levels around 300 hPa, close to the tropopause. Meanwhile, the convective available potential energy field (which is available as part of the ERA-Interim data set) shows modestly positive values of  $\sim 400 \text{ W m}^{-2}$  in the lightning region. Together, these results suggest that what we are seeing here is deep, upright (rather than slantwise) moist convection fed by the rapid lifting of high-entropy, low-level air originating over the warm sea surface temperatures of the northern Agulhas Current region. A further interesting aspect is the midlevel  $\theta_e$  minimum apparent in the cross-section of

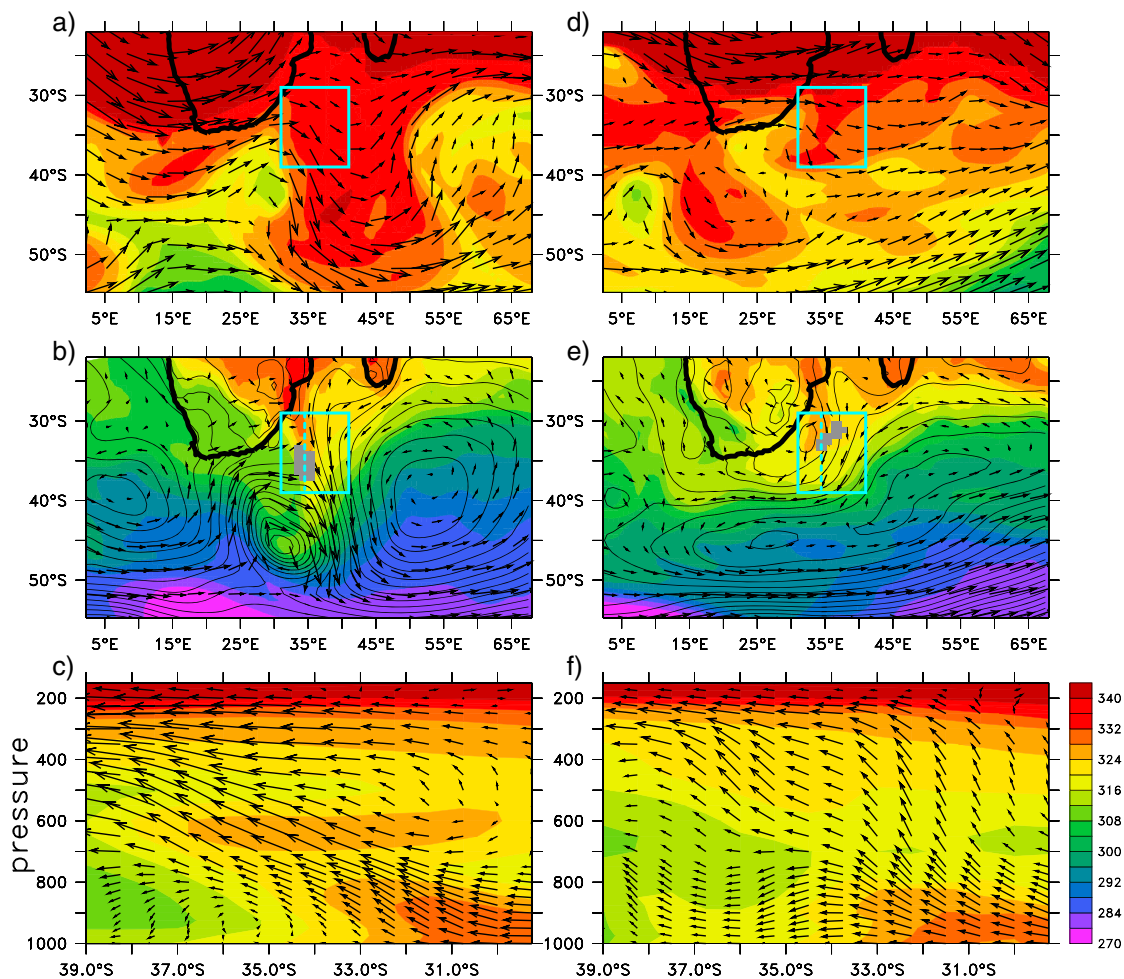


**Figure 7.** Synoptic conditions around the Agulhas Current region (cyan box) at 12 noon UTC on 15 October 2011 (left column) and 14 May 2011 (right column). Top row: potential temperature on the 2 PVU surface (shading, units of K) and 300 hPa horizontal wind (arrows). Middle row: equivalent potential temperature (shading, units of K) and horizontal wind (arrows) both averaged between 800 and 1000 hPa, and mean sea-level pressure (thin solid contours at 2 hPa intervals). Gray shading indicates regions of high lightning activity. Bottom row: north-south latitude-height cross-section through the region of high lightning activity. Shading shows equivalent potential temperature (units of K) and arrows show meridional-vertical velocity (pressure velocity has been multiplied by a negative factor accounting for the aspect ratio of the plot). The location of the sections is indicated by the dashed cyan lines in Figures 7b and 7e.

Figure 7c, which helps destabilize the column to moist convection. Inspection of the relevant fields suggests that this minimum is maintained by westerly advection of low-entropy air by the cyclonic circulation.

#### 4.2. Coastal Low (14 May 2011)

[19] The second case can be classified as a coastal low event, of the type often observed around South Africa [Reason and Jury, 1990]. This case is superficially rather different from the first, though as we will see, some fundamental aspects are common to both: specifically, while the synoptic-scale features are quite different in the two cases, the resulting subsynoptic-scale air flows end up being similar.

[20] At upper levels (Figure 7d), we see to the south of South Africa a deep poleward incursion of warm subtropical air which is bending anticyclonically and pinching off a weaker equatorward incursion of polar air. The result is a north-south dipole, with cyclonic flow near the southern tip

of South Africa and anticyclonic flow further south. This dipole can be traced down through all levels and all the way to the surface (Figure 7e). The cyclonic part of the dipole drives a westerly flow over the South African plateau; this airflow descends to sea level to the east of South Africa and generates a small-scale coastal depression there. On the eastward flank of the coastal low, the northerly flow again advects high- $\theta_e$  air into the Agulhas Current region. As in the previous example, note also the presence of a broad anticyclone to the east, which aids in conveying warm, moist air into the Agulhas Current region. The collision between northwesterly advection by the coastal low and northeasterly advection by the anticyclone conspires to sharpen the flow into a narrow, WCB-like structure which coincides with the region of high lightning intensity. A cross-section through this structure (Figure 7f) again shows that lightning is associated with rapid lifting of the high-entropy low-level air. The outgoing longwave radiation field again suggests

cloud tops near the tropopause, while convective available potential energy is again positive. Note also in this case the presence of a midtropospheric  $\theta_e$  minimum.

## 5. Summary

[21] We have studied the conditions and processes conducive to lightning over the Agulhas Current region and its retroreflection. We have found that lightning in this region is most common in the autumn but that there is significant lightning throughout the year. The mean winds in the region are typically northerly during thunderstorms. Composites of SLP and surface air temperature during days of lightning indicate an essential role for synoptic-scale wave trains and associated frontal systems passing through the region. Two individual cases of high lightning activity were studied in more detail, one involving a coastal low and another a cut-off low. While very different in their synoptic-scale configuration, both cases shared some fundamental features, namely a northerly low-level jet bringing very warm, moist air into the Agulhas Current region together with enough low-level convergence and lifting to trigger deep moist convection.

[22] We argue that ultimately the reason for high lightning frequency in the Agulhas Current region is the presence of anomalously warm sea surface temperatures associated with the boundary current itself. Synoptic-scale eddies produce fronts and lifting at all longitudes, but it is only in the Agulhas and other western boundary current regions that warm-sector low-level flow routinely acquires sufficient entropy to drive the intense moist convection required to generate lightning. In this sense, our study is complementary to previous work [Czaja and Blunt, 2011] which found that western boundary currents provide favorable environmental conditions for moist convection. Here we have focused on a direct proxy for convection, namely lightning, and shown that—at least in the Agulhas Current region—synoptic-scale systems play an essential role in generating and sustaining the conditions favorable for convection. Given the strong impact of deep convection on atmospheric stratification, these results may have wider implications for the atmospheric general circulation and the maintenance of the storm tracks. In future work we plan to focus on other western boundary current regions to determine whether synoptic-scale flows play a similar role there as in the Agulhas Current region.

[23] **Acknowledgments.** We thank Liesl Dyson of the University of Pretoria and Chris Reason from the University of Cape Town for helpful comments. LIS/OTD data were produced by the LIS/OTD Science Team (Principal Investigator, Dr Hugh J. Christian, National Aeronautics and Space Administration (NASA) / Marshall Space Flight Center (MSFC)) and were obtained from the Global Hydrology Research Center (GHRC) (<http://ghrc.msfc.nasa.gov/>). The NCEP reanalysis data were provided by the NOAA/OAR/ESRL PSD, Boulder, Colorado, USA (<http://www.esrl.noaa.gov/psd/>). We thank the World Wide Lightning Location Network (<http://wwlln.net>), a collaboration among over 50 universities and institutions, for providing the WWLLN lightning location data used in this paper.

## References

- Beal, L. M., W. P. M. De Ruijter, A. Biastoch, and R. Zahn (2011), On the role of the Agulhas system in ocean circulation and climate, *Nature*, 472 (7344), 429–436.
- Blamey, R. C., and C. J. C. Reason (2009), Numerical simulation of a mesoscale convective system over the east coast of South Africa, *Tellus A*, 61(1), 17–34.
- Blamey, R. C., and C. J. C. Reason (2012), Mesoscale Convective Complexes over Southern Africa, *J. Climate*, 25(2), 753–766.

- Boccippio, D. J., W. Koshak, R. Blakeslee, K. Driscoll, D. Mach, D. Buechler, W. Boeck, H. J. Christian, and S. J. Goodman (2000), The Optical Transient Detector (OTD): Instrument Characteristics and Cross-Sensor Validation, *J. Atmos. Ocean. Technol.*, 17(4), 441–458.
- Browning, K. A. (1986), Conceptual models of precipitation systems, *Weather Forecast.*, 1, 23–41.
- Cecil, D. J., S. J. Goodman, D. J. Boccippio, E. J. Zipser, and S. W. Nesbitt (2005), Three years of TRMM precipitation features. Part I: Radar, radiometric, and lightning characteristics, *Mon. Wea. Rev.*, 133(3), 543–566.
- Change, E. K. M. (2000), Wave packets and life cycles of troughs in the upper troposphere: Examples from the Southern Hemisphere summer season of 1984/85, *Mon. Wea. Rev.*, 128, 25–50.
- Christian, H. J., R. J. Blakeslee, D. J. Boccippio, W. J. Koshak, S. J. Goodman, and D. M. Mach (2000), Science data validation plan for the Lightning Imaging Sensor (LIS) Rep., US National Aeronautics and Space Administration, George C. Marshall Space Flight Center.
- Christian, H. J., et al. (2003), Global frequency and distribution of lightning as observed from space by the Optical Transient Detector, *J. Geophys. Res.*, 108(D1), 4005.
- Collier, A. B., A. R. W. Hughes, J. Lichtenberger, and P. Steinbach (2006), Seasonal and diurnal variation of lightning activity over southern Africa and correlation with European whistler observations, *Ann. Geophys.*, 24(2), 529–542.
- Czaja, A., and N. Blunt (2011), A new mechanism for ocean–atmosphere coupling in midlatitudes, *Q. J. R. Meteorol. Soc.*, 137(657), 1095–1101.
- Dee, D. P., et al. (2011), The ERA-Interim reanalysis: configuration and performance of the data assimilation system, *Q. J. R. Meteorol. Soc.*, 137(656), 553–597.
- Dirks, R. A., J. P. Kuettner, and J. A. Moore (1988), Genesis of Atlantic Lows Experiment (GALE): An Overview, *Bull. Am. Meteorol. Soc.*, 69(2), 148–160.
- Dowden, R., et al. (2008), World-wide lightning location using VLF propagation in the Earth-ionosphere waveguide, *IEEE Antennas Propag. Mag.*, 50(5), 40–60.
- Dyson, L. L. (2009), Heavy daily-rainfall characteristics over the Gauteng Province, *Water SA*, 35(5).
- Green, P. E., and J. D. Carroll (1978), *Analyzing Multivariate Data*, The Dryden Press, Hindsdale, USA, 519 pp.
- Hoskins, B. J., and K. I. Hodges (2005), A New Perspective on Southern Hemisphere Storm Tracks, *J. Climate*, 18(20), 4108–4129.
- Inatsu, M., and B. J. Hoskins (2004), The Zonal Asymmetry of the Southern Hemisphere Winter Storm Track, *J. Climate*, 17(24), 4882–4892.
- Jury, M., and N. Walker (1988), Marine boundary layer modification across the edge of the Agulhas Current, *J. Geophys. Res.*, 93(C1), 647–654.
- Kalnay, E., et al. (1996), The NCEP/NCAR 40-Year Reanalysis Project, *Bull. Am. Meteorol. Soc.*, 77(3), 437–471.
- Kodama, Y.-M., H. Okabe, Y. Tomisaka, K. Kotono, Y. Kondo, and H. Kasuya (2007), Lightning Frequency and Microphysical Properties of Precipitating Clouds over the Western North Pacific during Winter as Derived from TRMM Multisensor Observations, *Mon. Wea. Rev.*, 135(6), 2226–2241.
- Lee, S. and I. M. Held (1993), Baroclinic wave packets in models and observations, *J. Atmos. Sci.*, 50, 1413–1428.
- Mackerras, D., M. Darveniza, R. E. Orville, E. R. Williams, and S. J. Goodman (1998), Global lightning: Total, cloud and ground flash estimates, *J. Geophys. Res.*, 103(D16), 19791–19809.
- Mardia, K. V., J. T. Kent, and J. M. Bibby (1979), *Multivariate Analysis*, Academic Press, New York, 519 pp.
- Reason, C. J. C. (2001), Evidence for the Influence of the Agulhas Current on Regional Atmospheric Circulation Patterns, *J. Climate*, 14(12), 2769–2778.
- Reason, C. J. C., and M. R. Jury (1990), On the generation and propagation of the southern African coastal low, *Q. J. R. Meteorol. Soc.*, 116(495), 1133–1151.
- Reason, C. J. C., and A. Keibel (2004), Tropical Cyclone Eline and Its Unusual Penetration and Impacts over the Southern African Mainland, *Weather Forecast.*, 19(5), 789–805.
- Rodger, C. J., J. B. Brundell, and R. H. Holzworth (2009), Improvements in the WWLLN network: Bigger detection efficiencies through more stations and smarter algorithms, *Paper Presented at 11th IAGA Scientific Assembly Sopron*, Hungary.
- Rouault, M., A. M. Lee-Thorp, I. Anson, and J. R. E. Lutjeharms (1995), Agulhas Current Air-Sea Exchange Experiment, *S. Afr. J. Sci.*, 91(10), 493.
- Rouault, M., A. M. Lee-Thorp, and J. R. E. Lutjeharms (2000), The Atmospheric Boundary Layer above the Agulhas Current during Alongcurrent Winds, *J. Phys. Oceanogr.*, 30(1), 40–50.
- Singleton, A. T., and C. J. C. Reason (2007), A Numerical Model Study of an Intense Cutoff Low Pressure System over South Africa, *Mon. Wea. Rev.*, 135(3), 1128–1150.

- Taljaard, J. J. (1996), Atmospheric Circulation Systems, Synoptic Climatology and Weather Systems of South Africa. Part 6. Rainfall in South Africa, *South African Weather Service Report No. 32*, p. 100.
- Thorncroft, C. D., B. J. Hoskins, and M. E. McIntyre (1993), Two paradigms of baroclinic-wave life-cycle behaviour. *Q. J. R. Meteorol. Soc.*, *119*, 17–55.
- Tyson, P. D., and R. A. Preston-Whyte (2000), *The Atmosphere and Weather of Southern Africa*, Oxford University Press, Cape Town.
- Virts, K. S., J. M. Wallace, M. L. Hutchins, and R. H. Holzworth (2013), Highlights of a new ground-based, hourly global lightning climatology, *Bull. Am. Meteorol. Soc.*, doi:10.1175/bams-d-12-00082.1.
- Williams, E., and S. Stanfill (2002), The physical origin of the land–ocean contrast in lightning activity, *C. R. Phys.*, *3*(10), 1277–1292.